Available online at www.sciencedirect.com
SCIENCE DIRECT
Bioorganic & Medicinal Chemistry 14 (2006) 3002–3010
Bioorganic & Medicinal Chemistry

Mechanism of the Class I KDPG aldolase

Stephen W. B. Fullerton,[a,†] Jennifer S. Griffiths,[b] Alexandra B. Merkel,[a] Manoj Cheriyan,[c] Nathan J. Wymer,[b,‡] Michael J. Hutchins,[a] Carol A. Fierke,[c,a,*] Eric J. Toone[b,*] and James H. Naismith[a,*]

[a]*Centre for Biomolecular Sciences, The University of St Andrews, St Andrews, KY16 9ST, UK*
[b]*Department of Chemistry, Duke University, Durham, NC 27708, USA*
[c]*Chemistry Department, University of Michigan, Ann Arbor, MI 48109, USA*

Received 25 October 2005; revised 4 December 2005; accepted 9 December 2005
Available online 5 January 2006

Abstract—In vivo, 2-keto-3-deoxy-6-phosphogluconate (KDPG) aldolase catalyzes the reversible, stereospecific retro-aldol cleavage of KDPG to pyruvate and D-glyceraldehyde-3-phosphate. The enzyme is a lysine-dependent (Class I) aldolase that functions through the intermediacy of a Schiff base. Here, we propose a mechanism for this enzyme based on crystallographic studies of wild-type and mutant aldolases. The three dimensional structure of KDPG aldolase from the thermophile *Thermotoga maritima* was determined to 1.9 Å. The structure is the standard α/β barrel observed for all Class I aldolases. At the active site Lys we observe clear density for a pyruvate Schiff base. Density for a sulfate ion bound in a conserved cluster of residues close to the Schiff base is also observed. We have also determined the structure of a mutant of *Escherichia coli* KDPG aldolase in which the proposed general acid/base catalyst has been removed (E45N). One subunit of the trimer contains density suggesting a trapped pyruvate carbinolamine intermediate. All three subunits contain a phosphate ion bound in a location effectively identical to that of the sulfate ion bound in the *T. maritima* enzyme. The sulfate and phosphate ions experimentally locate the putative phosphate binding site of the aldolase and, together with the position of the bound pyruvate, facilitate construction of a model for the full-length KDPG substrate complex. The model requires only minimal positional adjustments of the experimentally determined covalent intermediate and bound anion to accommodate full-length substrate. The model identifies the key catalytic residues of the protein and suggests important roles for two observable water molecules. The first water molecule remains bound to the enzyme during the entire catalytic cycle, shuttling protons between the catalytic glutamate and the substrate. The second water molecule arises from dehydration of the carbinolamine and serves as the nucleophilic water during hydrolysis of the enzyme-product Schiff base. The second water molecule may also mediate the base-catalyzed enolization required to form the carbon nucleophile, again bridging to the catalytic glutamate. Many aspects of this mechanism are observed in other Class I aldolases and suggest a mechanistically and, perhaps, evolutionarily related family of aldolases distinct from the *N*-acetylneuraminate lyase (NAL) family.

1. Introduction

2-Keto-3-deoxy-6-phosphogluconate (KDPG) aldolase, a Class I aldolase of the Entner–Doudoroff glycolytic pathway, catalyzes the reversible cleavage of KDPG into the three-carbon units pyruvate and glyceraldehyde-3-phosphate (Scheme 1).[1] The mechanism of both aldol addition and elimination proceeds through an imine, formed with an active site lysine. In both the synthetic and cleavage reactions, a requisite series of proton transfers is facilitated by catalytically relevant acidic and basic side chains.

The enzymatic aldol reaction is highly efficient, regioselective and, in many cases, shows high facial stereoselectivity; for these reasons aldolases have long been of interest to the synthetic community.[2–5] However, the relatively narrow substrate specificities of many aldolases limit their utility in chemical synthesis. The synthetic community has long sought to enhance the utility of synthetically useful enzymes by broadening or shifting substrate specificities through protein modification but, in general, the ability to employ rational redesign of enzyme active sites remains limited.[6] By contrast, so-called

Keywords: KDPG aldolase; Class I mechanism; Schiff base; Carbinolamine.
* Corresponding authors. Tel.: +1 919 681 3484; fax: +1 919 668 5483 (E.J.T.); tel.: +1 734 936 2678; fax: +1 734 647 4865 (C.A.F.); tel.: +44 1334 463792; fax: +44 1334 463808 (J.H.N.); e-mail addresses: fierke@umich.edu; Eric.Toone@duke.edu; naismith@st-and.ac.uk
† Present address: Department of Biochemistry, Adrian building, University of Leicester, Leicester LE17RH, UK.
‡ Present address: zuChem, Inc., Peoria, IL 61604, USA.

0968-0896/$ - see front matter © 2005 Elsevier Ltd. All rights reserved.
doi:10.1016/j.bmc.2005.12.022

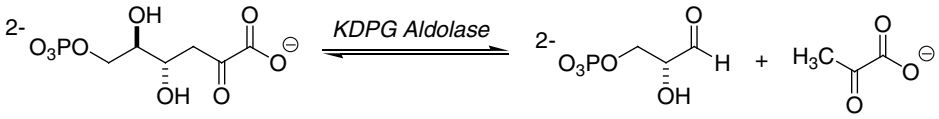

Scheme 1. KDPG aldolase reaction.

diversity-based approaches such as directed evolution have produced several notable successes and offer an alternative methodology for improving the utility of enzymes as synthetic catalysts.[6–9] In addition to providing useful synthetic tools, directed evolution facilitates an understanding of structure–function relationships in protein catalysis, by providing structural solutions to pre-determined mechanistic problems. The interpretation of such experiments requires detailed structural knowledge of the enzyme active site, including the substrate recognition regions. As part of a wider program of protein engineering, we have investigated the structural basis of substrate specificity and the mechanism of catalysis of KDPG aldolase using native and mutant proteins from both *Thermotoga maritima* and *Escherichia coli*.

A number of studies designed to elucidate the molecular mechanism of enzymatic aldol addition and the structural basis of stereoselectivity have been reported. Most of them have considered Class I aldolases, although several studies of zinc-dependent Class II enzymes have recently been reported.[10–13] The initial structures of Class I aldolases located the active site lysine, a residue conserved in position on β6 strand of the barrel across the entire enzyme family regardless of substrate. The exception is transaldolase where the lysine in located in the β4 strand.[14] Later studies reported substrate-bound co-complexes for aldolases from several sources, in particular fructose-1,6-diphosphate aldolase and transaldolase.[14–16] Yet even with these structures, a detailed molecular mechanism of imine formation, nucleophilic addition to an electrophilic aldehyde, and product release—processes that require the sequential provision and abstraction of several protons—remained elusive. The next important advance toward the elucidation of a molecular mechanism came with the structure of a carbinolamine covalent intermediate at the active site of the *E. coli* KDPG aldolase.[17] The structure identifies Glu 45 as the only plausible general acid/base, although the orientation of the carbinolamine precludes direct deprotonation by the glutamate.

D-2-Deoxyribose-5-phosphate aldolase (DERA), a Class I aldolase that catalyzes the reversible condensation of acetaldehyde and glyceraldehyde-3-phosphate, has also been the subject of extensive synthetic and mechanistic studies. Recently, Wilson and Wong proposed a molecular mechanism for DERA catalysis that invokes the cyclic relay of protons between water and three protein residues during turnover.[18] Although the evidence for the proposed mechanism is compelling, the proposed mechanism cannot be general as several key residues are not conserved in other aldolases. A proton shuttling mechanism has been proposed in FBP aldolase[19] but there is still an ongoing debate as to its precise nature.[20]

We and others have utilized the aldolases of the Entner–Doudoroff pathway as synthetic catalysts.[21–23] In the course of our efforts to understand the molecular basis of both catalysis and stereoselectivity, we have previously reported structures of the wild-type *E. coli* KDPG aldolase and an evolved mutant showing altered substrate specificity.[24] Here, we report the structures of *T. maritima* KDPG aldolase[25] covalently modified as the Schiff base complex with pyruvate and a catalytically incompetent *E. coli* KDPG aldolase complex with a pyruvyl carbinolamine. We propose a mechanism for catalysis reminiscent of that proposed for DERA, including a crucial role for an active site water molecule. There are, however, important differences between the proposals.

In both aldolases, an anion is bound—in *T. maritima* a sulfate and in *E. coli* a phosphate—in identical loci, despite being crystallized under different conditions. By assuming that these anions reveal the substrate phosphate binding site, we have created a model of KDPG-bound aldolase. The model may provide a rationalization for the unusual trimeric structure of the KDPG aldolases.

2. Results and discussion

2.1. Overall structures

The folds of both *T. maritima* and *E. coli* KDPG aldolases are unchanged from previous descriptions of the enzyme, displaying the classic α/β barrel structure.[17,24,26] The monomers of *T. maritima* and *E. coli* enzymes superimpose with an RMS deviation for 188 matching Cα atoms of 1.5 Å. There are slight differences between the structures reflecting rigid body movement of the secondary structure elements. The most obvious differences are in the loop to the C-terminal helix and at the N-terminus, both of which are shorter in *T. maritima* than the *E. coli* enzyme. The quaternary structure of the *T. maritima* trimer is the more compact of the two enzymes, manifested in the closer contact in *T. maritima* between the open C-terminal end of the barrel from one monomer and the loop from residues 143 to 152 in the other. The enzyme from *Pseudomonas putida*[26] superimposes with an RMS deviation of 1.5 Å for 183 matching Cα atoms. Superposition of the various trimers increases the deviation to 2.0 Å, reflecting the subtly different arrangements seen for the trimer in all crystal structures. In *T. maritima*, Glu 40 and Lys 129 are conserved in position and sequence with Glu 45 and Lys 133 in the *E. coli* enzyme.

2.2. Schiff base structure of *T. maritima* enzyme

There are two trimers (six monomers) in the unit cell structure of *T. maritima* KDPG aldolase: our descrip-

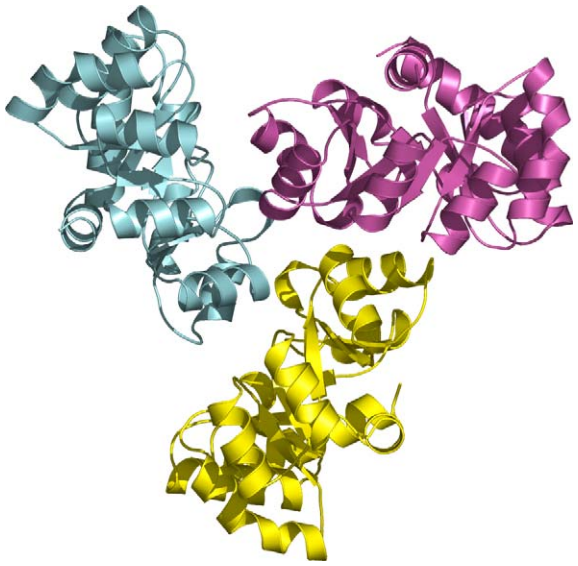

Figure 1. The structure of the KDPG aldolase is a trimer.

tion focuses on one of these trimers (monomers A, B, and C) (Fig. 1). The trimers are essentially identical, except for minor differences in side-chain orientations and water structure. As the structure was refined, the electron density clearly showed a pyruvate bound to Lys 129 as the Schiff base (Fig. 2). The orientation of the pyruvate carboxylate group is the same as that described previously for the carbinolamine structure,[17] forming a bidentate hydrogen bond to Arg 17 and the highly conserved Thr 69. The putative catalytic base, Glu 40, is remote from the key atoms of the Schiff base ε-N (4.3 Å), C2 (4.7 Å), and C3 (5.8 Å). The methyl group (C3) of pyruvate points toward the highly conserved Phe 131, part of the characteristic GxxxωKφFP motif that includes the key catalytic lysine (ω is a hydrophobic residue (L, F, I, M, V, and C) and φ is a bulky hydrophobic residue (F, I, V, and L)). Phe 131 caps the pyruvate methyl group and likely limits the degree of substitution tolerated by the enzyme at the C3 position.

A sulfate ion is bound 7.7 Å from C3 along the channel at the C-terminal end of the barrel near the so-called 'standard phosphate binding motif' common to many α/β-barrel enzymes.[27] In *T. maritima*, amide nitrogens of Gly 157, Gly 158, Val 159, Ser 179, and the Ser 179 hydroxyl group form the pocket. A sulfate is bound at an identical position in the *P. putida* structure. The Gly 157-Gly 158 pair allows a very tight turn in the loop region connecting strands β7 and α8, and is found in over 95% of all KDPG aldolases. A water molecule (W1) is located less than 3.1 Å from C2, bridging the side chains of Glu 40 and Lys 129, and in a position consistent with an origin in elimination from the pyruvyl carbinolamine. A second water molecule (W2) forms hydrogen bonds to W1, Thr 156, and Glu 40 (Fig. 2). W2 is also found in the native *E. coli* carbinolamine structure[17] where it bridges the catalytically relevant Glu 45 and Lys 133.

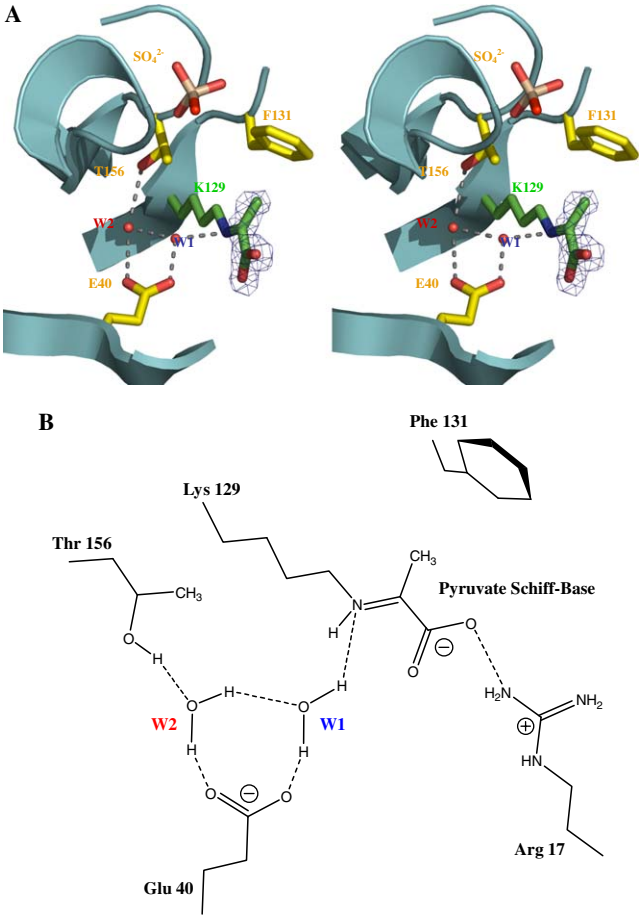

Figure 2. The active site of *T. maritima*. (A) The catalytic lysine, Lys 129, bound to pyruvate as a Schiff base is highlighted in green. The two key waters W1 (labeled in blue) and W2 (labeled in red) are shown. The Fo-Fc omit map contoured at 4σ is shown for the Schiff base. The experimentally located SO_4^{2-} ion, which binds at the standard phosphate binding site, is shown and labeled. Apart from Lys 129, carbon atoms are colored yellow, oxygen atoms are colored red, and nitrogen blue. (B) An alternative representation emphasizing the chemical properties of the active site.

2.3. E45N *E. coli* KDPG structure

We wish to confirm that the E45N mutation did not perturb the active site in some way which could explain the low activity of this mutant. On solving the structure we found that the A subunit (supplementary Figure) shows additional density consistent with a carbinolamine intermediate, although at less than full occupancy. There is some disorder at the catalytic lysine, as a result we did not refine the structure with the carbinolamine present.[17] The additional carbinolamine density in the mutant *E. coli* KDPG aldolase is essentially identical to that previously observed in the native structure.[17] A phosphate ion in this structure superimposes with the sulfate in the native *E. coli* enzyme[17] and the *T. maritima* enzyme. Superposition of the *T. maritima* enzyme and the two *E. coli* carbinolamine structures (E45N and native[17]) reveals that the water molecule, W1, seen in *T. maritima* is absent. The pyruvyl carbinolamine hydroxyl group would be only 2.1 Å away, suggesting one would repel the other

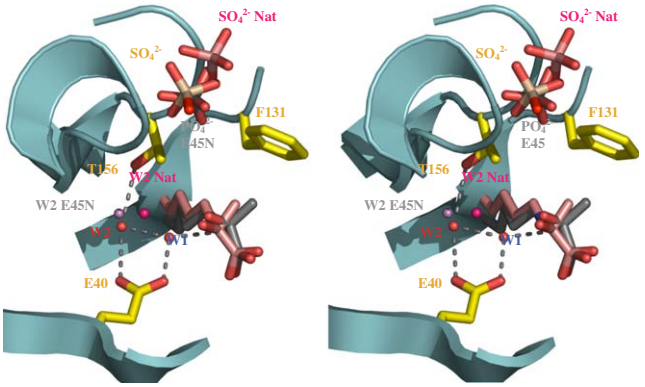

Figure 3. Lys 133 from *E. coli* native (carbon colored pink) and *E. coli* E45N (carbon colored grey) superimposed upon the active site of *T. maritima*. The color scheme for the remainder of the figure is as in Figure 2. W1 is absent in both carbinolamine structures, due to the presence of the carbinolamine hydroxyl group. However, both carbinolamine structures have an equivalent water molecule (shown and labeled) to the W2 identified in the *T. maritima* Schiff base complex. The phosphate (E45N) and sulfate (native) of the carbinolamine structures superimpose with the sulfate ion found in *T. maritima*.

(Fig. 3). This is consistent with our assertion that W1 arises from the hydroxyl of the carbinolamine as a result of the elimination of water during Schiff base formation. In the E45N mutant, a water molecule is also found close to the W2 position but, likely due to the mutation, its position is shifted by over 2.0 Å (Fig. 3).[17]

2.4. Model of the substrate in the *T. maritima* structure

The orientation of pyruvate in the enzyme active site first observed by Allard et al.[17] is conserved both in the pyruvyl carbinolamine adduct of a catalytically incompetent enzyme (E45N enzyme) and in the pyruvyl imine adduct of the native *T. maritima* protein. Based on these three structures and the positioning of a complex anion (phosphate, sulfate) in structures from both sources, we propose a bound model of an open-chain KDPG (Fig. 4). A model of KDPG was superimposed on the pyruvyl Schiff base and carbinolamine structures, with C1, C2, and C3 matching the experimentally determined positions. The remainder of the sugar was modeled into the protein by adjusting the torsion angles to −169° (C3–C4); −176° (C4–C5), and +177° (C5–C6). The C6–O6 bond adopts a gauche conformation, with a dihedral angle of −57°. In this orientation, the phosphate of the substrate overlaps almost exactly with the experimental positions of the anions (Fig. 4).

In the model of the full-length gluconyl Schiff base, both W1 and W2 are placed in positions equivalent to those observed in the pyruvyl Schiff base complex. We suggest that during product release, W1 adds across the imine to form the carbinolamine intermediate. Although O4 of the sugar is close to the conserved Thr 156, it is too far (4.7 Å) for a direct hydrogen bond. However, in all structures there is a water network which could bridge O4 and Thr 156. The hydroxyl located on carbon five (O5) of the sugar makes a hydrogen bond (3.1 Å) with the backbone carbonyl of Ala 143 from the neighboring subunit (Fig. 4).

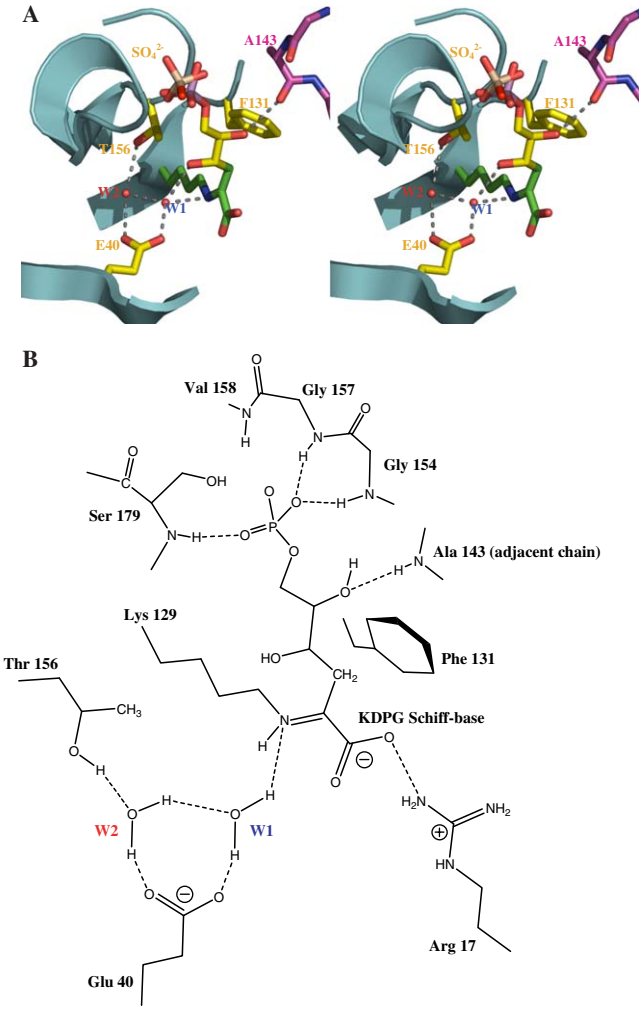

Figure 4. The model for KDPG bound to the enzyme. (A) The modeled carbon atoms of KDPG are colored yellow, the experimentally located atoms are colored as in Figure 2. The contact with the neighboring subunit (carbon colored purple) is shown. The modeled phosphate of the substrate closely overlaps with the experimentally located sulfate. (B) A chemical representation of KDPG at the enzyme active site.

Similar models of substrate binding are easily constructed for the *E. coli* and *P. putida* enzymes. These models, however, do not predict the contact between O5 and the backbone of the neighboring subunit seen in the *T. maritima* model. This difference may reflect the greater separation of monomers in the *E. coli* and *P. putida* structures relative to the *T. maritima* protein. As we have noted, the arrangement of monomers in the trimer depends on crystallization conditions, even for the same protein. While these observations are not evidence that the *E. coli* enzyme can form the same inter-subunit contact as the *T. maritima* enzyme per se, they do offer a possible explanation for the unique trimeric arrangement of monomers of the KDPG aldolases.

2.5. Implications for catalysis by the *E. coli* enzyme

Aldol addition by KDPG aldolase involves sequential formation of a pyruvyl carbinolamine, dehydration to the imine, and enolization to the nucleophilic enamine

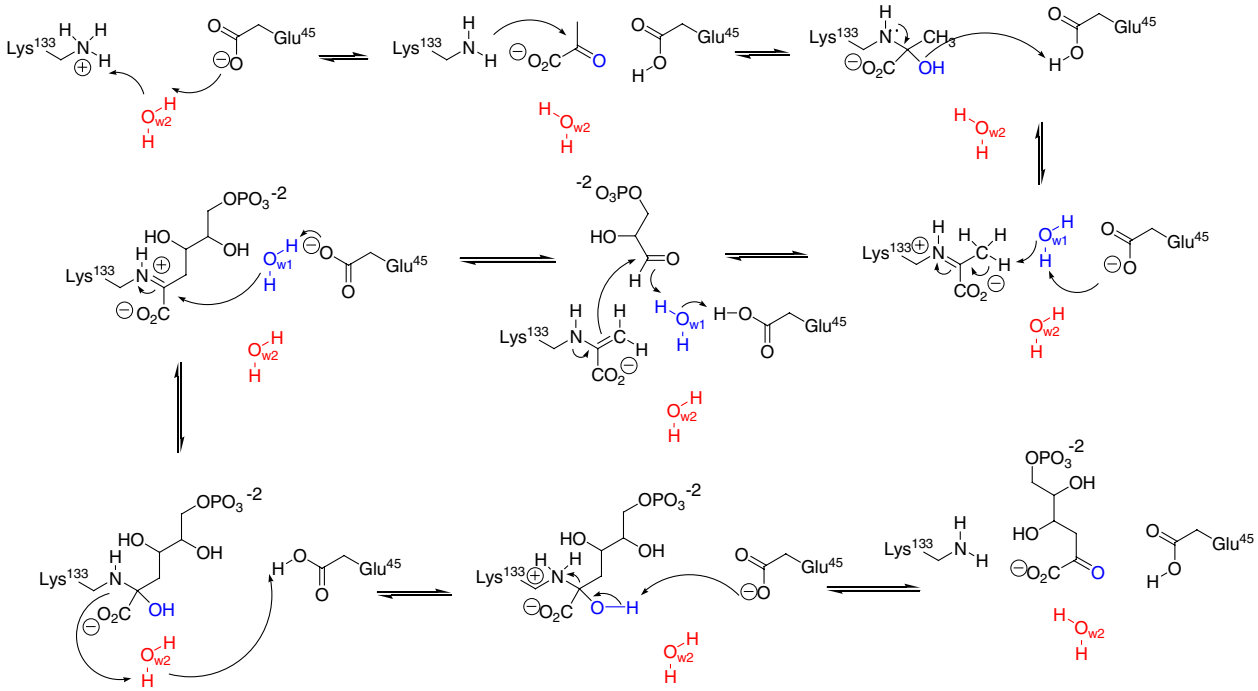

Scheme 2. The mechanism of KDPG Aldolase, numbering as *E. coli.* For *T. maritime* Glu 40 and Lys 128 are the two protein residues.

(Scheme 2). Addition to an aldehydic electrophile results in a gluconyl imine which is, in turn, hydrated to the corresponding carbinolamine and released as the keto-acid product. Catalysis is mediated by a nucleophilic amine and by a series of proton transfers to and from a highly conserved glutamate that serves, in turn, as both a general acid and a general base.

Formation of the initial carbinolamine requires a significant population of the deprotonated form of Lys 133. The pK_a of lysine ε-amino group can be diminished by both inclusion in a low dielectric media and the presence of a proximal positively charged residue; both mechanisms may be operative here. The central pore of the β-barrel is relatively hydrophobic and inclusion of substrate within this pore should further dehydrate the pore thus lowering the pK_a of the catalytic lysine. The KDPG aldolases contain a conserved arginine residue (R49), which, although somewhat removed from the catalytic lysine (~5 Å), is important for catalysis (Toone and Fierke, unpublished results). Together, these effects presumably provide a lysine residue sufficiently nucleophilic to affect catalysis.

From a comparison of both structures and sequence alignments it seems clear that only the absolutely conserved Glu 45 is positioned to function as the acid/base. On the other hand, Glu 45 forms direct contacts only to O2 of the carbinolamine intermediate; Glu 45 cannot form contacts to the catalytic lysine, to C3 of either the pyruvyl or gluconyl intermediates, or to O4 of the gluconyl carbinolamine or imine. This apparent separation of the putative acid/base from those sites requiring proton donation and abstraction precludes direct proton transfer. This represents a recurring challenge to the elucidation of aldolase mechanism.

In the proposed DERA mechanism, a triad of Lys 201, Asp 102, and a bridging water acts in concert to shuttle protons on and off both the substrate and the catalytic lysine during turnover.[18] However, this mechanism cannot be generalized to other aldolases, since DERA alone has a second lysine relevant to catalysis. Furthermore, KDPG (and other) aldolases lack a potential base near the position occupied by Asp 102 in DERA (Ile 92 in KDPG aldolase). The mechanism proposed for DERA catalysis[18] does, however, suggest that water-mediated proton transfer should be considered for other aldolases. Our analysis of KDPG aldolase structures highlighted two water molecules relevant to catalysis: W1, in position to arise from elimination of water from a carbinolamine intermediate, and W2, which is always present. W2, which has previously been suggested as relevant to catalysis,[17] bridges the catalytic lysine and glutamate residues in both the apo and carbinolamine structures, allowing glutamate to effect proton transfer during carbinolamine formation (Scheme 2). The observation of the carbinolamine intermediate in the catalytically incompetent *E. coli* E45N mutant argues that proton transfer to solvent during carbinolamine synthesis is sufficiently facile to support the reaction. In the second step, we propose that W2 and Glu 45 act in concert to transfer a proton to the carbinolamine hydroxyl, triggering the elimination of water (W1) and producing the imine (Scheme 2).

Prior to aldol addition, the Schiff base must be enolized to the nucleophilic enamine, a process that requires deprotonation of pyruvyl imine at C3. Both the Schiff base and carbinolamine structures place the conserved glutamate some 6 Å from this carbon, too far for direct proton transfer and there is no chemically reasonable appropriately positioned alternate residue. Rather than

direct transfer, water mediation could play a role here also. In the Schiff base complex W1, which arises during Schiff base formation, bridges C3 (4.0 Å) and Glu 45 (2.6 Å). Movement of W1 by less than 1.0 Å would facilitate efficient proton transfer from pyruvyl C3 to Glu 45. In contrast, the alternate proposal, rotation of the lysine Schiff base to bring C3 within hydrogen bonding distance of Glu 45, dramatically alters the recognition environment of the pyruvyl carboxylate group, creating several van der Waals clashes and seems unlikely.

During aldol addition, C3 of the pyruvyl enamine attacks the aldehyde of glyceraldehyde-3-phosphate. As the hybridization of the aldehydic carbon changes, the incipient oxyanion is protonated to form the alcohol. From our modeled substrate complex, a protonated Glu 45 would be able to transfer a proton to this oxygen using the same bridging W1 (Scheme 2). In the reverse reaction, glutamate would abstract a proton from O4, again via a bridging water, triggering retroaldol cleavage.

2.6. Contrast with DERA aldolase mechanism

The structures of native DERA bound as the carbinolamine intermediate and of a mutant variant trapped as the Schiff base intermediate first highlighted the role of bridging waters in the aldolase mechanism.[18] In both DERA and KDPG aldolase, the Schiff base-forming lysine is found on the β-6 strand, the standard phosphate binding site is used, and the substrates bind in an extended conformation. The difference in the enzyme mechanism between the two enzymes appears to lie in the positions of the basic residues. The two residues implicated in proton transfer in DERA, Asp 102 and Lys 201, are occupied in space by isoleucine and cysteine (C159), respectively, in KDPG aldolase. While cysteine could conceivably function in proton transfer, the C159A mutation in *E. coli* KDPG aldolase retains high activity (k_{cat}/K_M = 360,000 M^{-1} s^{-1}), suggesting that this is unlikely. Similarly, the glutamate residue proposed as the key general acid/general base during KDPG aldolase catalysis is replaced by cysteine in DERA. Since the DERA C47A mutant retains significant activity (k_{cat}/K_M = 43,000 M^{-1} s^{-1}), here again it is unlikely that this side-chain functions as a general base.[18] Additionally, in KDPG aldolase the activity of the E45N mutant is significantly impaired (k_{cat}/K_M = 3 M^{-1} s^{-1}).

One of the two water molecules proposed as catalytically relevant in KDPG aldolase (W1) is not visible in the mutant K201L DERA Schiff base structure. There is another water molecule in mutant DERA structure but it occupies the hydrophilic hole previously filled by the Nz atom of the wild-type enzyme. We suggest this position of the water molecule is an artifact of the mutant structure. We suggest that in the native DERA the water molecule created by Schiff base formation plays the same role as W1 in KDPG aldolase. The alternative is that this water is expelled from the active site re-entering to complete the reaction, no obvious tunnel exists in the DERA structures.

This mechanistic paradigm differs markedly from that proposed for the *N*-acetylneuraminate lyase (NAL) family of Class I aldolases, a group that includes 2-keto-3-deoxygluconate (KDG) aldolase. This group of proteins includes an absolutely conserved tyrosine roughly 4 Å from the pyruvate C3 moiety, and no additional conserved acidic or basic residues. Rather, the NAL family is proposed to function through substrate catalysis, with the substrate carboxylate moiety acting as the general acid/base through the intermediacy of the tyrosine hydroxyl group.[28–31] While a bridging water does not appear necessary for proton shuttle during sialic acid formation/hydrolysis, a water molecule that is at least in position to participate in proton shuffling is observed in the *Sulfolobus* KDG aldolase and may account for the promiscuous substrate specificity of this enzyme.

Throughout, we have invoked a role for key water residues in the kinetic mechanism of the aldolase-catalyzed reaction. It is important to note that these same water molecules could play important roles in ligand binding and substrate recognition. Such water-mediated recognition would further facilitate the ready evolution of aldolases specific for a wide variety of substrates from a common precursor fold.

3. Conclusions

We have proposed a detailed mechanism for KDPG aldolase. This mechanism may be general for aldolases that require only a nucleophilic lysine and a glutamate/aspartate acid/base. Two water molecules (W1 and W2) are crucial to the mechanism. The first is present throughout turnover, acting as a proton relay during both imine and carbinolamine formation. The second water is transient, arising from the dehydration of the intermediate carbinolamine and consumed by the hydrolysis of the imine, and relays protons during imine enolization and the formation of the carbon nucleophile. Such water-mediated proton relay during carbinolamine formation was first suggested for DERA.[18] Here, we hypothesize that DERA, like KDPG aldolase, uses a second water molecule (created during imine formation) to relay protons during imine/enamine interconversion.

DERA and KDPG aldolase use different residues in different locations to achieve catalysis; the mechanisms are thus not completely equivalent. This observation is surprising since key residues are typically conserved in both space and sequence in such closely related enzymatic activities. There may, in fact, be no completely general mechanism for the enzymatic aldol reaction. What does appear to be essential and conserved is acid/base catalysis mediated by water and the location of the nucleophilic lysine within the barrel. On the other hand, the position and nature of the acid/base with respect to the lysine is flexible since water-mediated proton relays can support proton transfer to and from a variety of positions. Presumably, the precise positioning of these residues facilitates control over the stereochemical course of the reaction. We note that the catalytic 38C2 antibody is an efficient aldolase.[32] This efficiency stands

in contrast to the general observation that catalytic antibodies are much less active than their enzyme counterparts. Similarly a KDPG aldolase mutant in which the lysine residue is moved to an alternative position within the barrel retains activity, however it shows altered substrate and stereoselectivities.[24] We continue our evolutionary and mechanistic studies of the pyruvate aldolases and will report our results in due course.

4. Experimental

4.1. Materials

Restriction endonucleases and T4 DNA ligase were obtained from New England Biolabs. Oligonucleotides were purchased from IDT (Integrated DNA Technologies, Inc.), *Pfu* DNA polymerase from Stratagene, anion exchange POROS HQ media from Amersham Biosciences, and His-bind nickel affinity resin from Novagen. XL 10-Gold and BL-21(DE3) strains of *E. coli* were used for cloning and over-expression, respectively. The DF71 cell line was a gift from the *E.coli* Genetic Stock Center at Yale University. UV kinetic assays were performed on a Hewlett–Packard 8453 UV–vis spectrophotometer fitted with a thermocoupled cuvette holder. Crystal data was obtained using an ADSC Quantum-4 CCD detector.

4.2. *T. maritima* KDPG aldolase

The protein was expressed from the previously described pTM-eda plasmid in BL21(DE3) cells.[25] Protein production was induced by addition of 0.5 mM IPTG at $OD_{600} = 0.8$. Cells were harvested by centrifugation after 3 h and lysed by sonication in the presence of 0.1 mM PMSF. Cell debris was removed by centrifugation and the supernatant was heated to 70 °C for 3 min. The supernatant was further purified by anion exchange chromatography using POROS HQ media (Amersham Biosciences). Crystals of protein were obtained after 3 days by the hanging drop methodology at 22 °C. A 2 μL aliquot of 5 mg mL^{-1} protein in 50 mM Tris (pH 7.0) was mixed with 2 μL of a reservoir solution containing 0.075 M sodium acetate, 0.1 M ammonium sulfate, and 27% w/v PEG 4000 at pH 4.6. Crystals were cryoprotected in a solution containing 50% PEG 4000K and identical salt concentrations to the reservoir. Data were collected at the ESRF ID14-2 using an ADSC Quantum-4 CCD detector. A data set to 1.9 Å was collected at a wavelength of 0.932 Å. Data collection statistics are summarized in Table 1. The structure was solved by molecular replacement with the *E. coli* KDPG aldolase structure.[24] The structure was refined using REFMAC5[33,34] and rebuilt using O;[35] the final statistics on the model are given in Table 1. The Fo-Fc density maps clearly showed that a Schiff base complex between Lys 129 and pyruvate was formed. Pyruvate was built using PRODRG and incorporated into the refinement.

4.3. Site-directed mutagenesis of *E. coli* KDPG aldolase

The mutant of the *E. coli* enzyme was constructed in pET-30b with the following primers (mutated bases underlined): E45N For (5′-GCT GGT GGG GTG CGC GTT CTG AAC GTG ACT CTG CGT ACC GAG TG-3′) and E45N Rev (5′-CAC TCG GTA CGC AGA GTC ACG TTC AGA ACG CGC ACC CCA CCA GC-3′); C159A For (5′ - GGT CCG TTT CGC CCC GAC GGG TGG TAT TTC-3′), and C159A Rev (5′-GAA ATA CCA CCC GTC GGG GCG AAA CGG ACC-3′). Details of the PCR conditions have been previously described.[24] Presence of the mutation was confirmed by sequencing of the resulting plasmid.

4.4. *E. coli* E45N KDPG aldolase

The protein at 4 mg mL^{-1} was crystallized by vapor diffusion against 20% PEG 6K, similar to the native *E. coli* enzyme.[24] A data set to 1.4 Å was collected at wavelength of 0.932 Å. Data collection statistics are summarized in Table 1. The structure was solved by molecular replacement with the *E. coli* KDPG aldolase structure.[24] The structure was refined using REFMAC5[33,34] and rebuilt using O;[35] the final statistics on the model are given

Table 1. Crystallographic data

	T. maritima	*E. coli* E45N
Resolution (Å)	33–1.9	40–1.55
High resolution shell	2.0–1.9	1.59–1.55
Cell dimensions	$a = 42.6$ Å, $b = 101.1$ Å, $c = 124.6$ Å, $\alpha = \gamma = 90°$, $\beta = 97.2°$	$a = 54.5$ Å, $b = 84.2$ Å, $c = 132.4$ Å, $\alpha = \beta = \gamma = 90°$
Spacegroup	$P2_1$	$P2_12_12_1$
R_{merge}	7.2% (29.6)	7.5% (35.6%)
Completeness	94.3% (94.2%)	99.4% (98.8%)
Redundancy	4.0 (3.9)	3.4 (3.2)
Refinement		
R_{factor}	18.8% (20.0%)	16.7% (16.5%)
R_{free}	23.7% (28.2%)	21.7% (24.4%)
RMS deviation		
Bonds	0.016	0.017
Angles	1.53	1.7
Core Ramachandran (%)	95.3	96%
PDB code	1wa3	2c0a

in Table 1. The Fo-Fc density maps clearly indicate there may be a partially occupied carbinolamine bound at Lys 129. We presume this arises from the cell milieu and is simply in equilibrium with free pyruvate. The absence of the E45, prevents the formation of the Schiff base.

4.5. Kinetic characterization of *E. coli* E45N KDPG aldolase

In order to prevent wild-type KDPG aldolase contamination, the E45N mutant was expressed in a cell line lacking endogenous KDPG aldolase. The DF71 cell line [*lacI22* LAM$^-$ e14$^-$ *eda-1 relA1 SpoT1 thi-1*] was obtained as a generous gift from the *E. coli* Genetic Stock Center at Yale University.[36] The E45N mutation was introduced into the previously described pUC-ECEDA2 using the same E45N For and E45N Rev primers described above.[37] The resulting pUC-ECEDA2(E45N) plasmid was transformed into DF71 cells. A 50 mL Terrific Broth/carbenicillin (60 μg mL^{-1}) culture was inoculated with a single colony and grown for 12 h at 37 °C and 220 rpm. A 1 L Terrific Broth/carbenicillin culture was subsequently inoculated with 10 mL of this overnight culture and grown to $OD_{600} = 0.8$ at 37 °C and 220 rpm. The culture was induced with 1 mM IPTG for 4 h at 37 °C and then pelleted. The cells were disrupted by French press and cell debris removed by centrifugation. The protein was purified via Ni^{2+} affinity chromatography (Novagen) and dialyzed against 3× 2 L of 20 mM HEPES (pH 7.5) to remove imidazole.

KDPG aldolase activity was determined by utilizing the coupled assay with sc l-lactic dehydrogenase.[38] Briefly, HEPES (50 mM, pH 7.5), NADH (0.1 mM), KDPG (0.4–16 mM), and L-lactic dehydrogenase (EC 1.1.1.27 Type II from rabbit muscle, 105 U) were combined in a total volume of 1 mL. KDPG aldolase (20 μM) was added to initiate the reaction and the disappearance of reduced cofactor was monitored for 10 min by measuring the absorbance at 340 nm. KDPG aldolase activity was determined from the initial slope of the absorbance versus time curve, and kinetic parameters were determined by fits of the Michaelis–Menten equation to using Origin 5.0 (Microcal).

Acknowledgments

This work was supported by the National Institutes of Health (GM61596 to E.J.T and C.A.F.) and the Wellcome Trust (J.H.N.). J.H.N. is a Biotechnology Biological Science Research Council career development fellow. J.S.G., M.C., and N.J.W. were supported in part by the NIH Chemistry-Biology Interface Training Grant.

Supplementary data

Supplementary data associated with this article can be found, in the online version, at doi:10.1016/j.bmc.2005.12.022.

References and notes

1. Conway, T. *FEMS Microbiol. Rev.* **1992**, *103*, 1–28.
2. Fessner, W. D.; Walter, C. *Bioorg. Chem.* **1997**, *184*, 97–194.
3. Seoane, G. *Curr. Org. Chem.* **2000**, *4*, 283–304.
4. Silvestri, M. G.; Desantis, G.; Mitchell, M.; Wong, C.-H. *Top. Stereochem.* **2003**, *23*, 267–342.
5. Wymer, N.; Toone, E. J. *Curr. Opin. Chem. Biol.* **2000**, *4*, 110–119.
6. Hult, K.; Berglund, P. *Curr. Opin. Biotechnol.* **2003**, *14*, 395–400.
7. Joerger, A. C.; Mayer, S.; Fersht, A. R. *Proc. Natl. Acad. Sci. U.S.A.* **2003**, *100*, 5694–5699.
8. Williams, G. J.; Domann, S.; Nelson, A.; Berry, A. *Proc. Natl. Acad. Sci. U.S.A.* **2003**, *100*, 3143–3148.
9. Fong, S.; Machajewski, T. D.; Mak, C. C.; Wong, C. H. *Chem. Biol.* **2000**, *7*, 873–883.
10. Joerger, A. C.; Mueller-Dieckmann, C.; Schulz, G. E. *J. Mol. Biol.* **2000**, *303*, 531–543.
11. Kroemer, M.; Merkel, I.; Schulz, G. E. *Biochemistry* **2003**, *42*, 10560–10568.
12. Cooper, S. J.; Leonard, G. A.; McSweeney, S. M.; Thompson, A. W.; Naismith, J. H.; Qamar, S.; Plater, A.; Berry, A.; Hunter, W. N. *Structure* **1996**, *4*, 1303–1315.
13. Plater, A. R.; Zgiby, S. M.; Thomson, G. J.; Qamar, S.; Wharton, C. W.; Berry, A. *J. Mol. Biol.* **1999**, *285*, 843–855.
14. Jia, J.; Schorken, U.; Lindqvist, Y.; Sprenger, G. A.; Schneider, G. *Protein Sci.* **1997**, *6*, 119–124.
15. Dalby, A.; Dauter, Z.; Littlechild, J. A. *Protein Sci.* **1999**, *8*, 291–297.
16. Thorell, S.; Schurmann, M.; Sprenger, G. A.; Schneider, G. *J. Mol. Biol.* **2002**, *319*, 161–171.
17. Allard, J.; Grochulski, P.; Sygusch, J. *Proc. Natl. Acad. Sci. U.S.A.* **2001**, *98*, 3679–3684.
18. Heine, A.; DeSantis, G.; Luz, J. G.; Mitchell, M.; Wong, C. H.; Wilson, I. A. *Science* **2001**, *294*, 369–374.
19. Heine, A.; Luz, J. G.; Wong, C. H.; Wilson, I. A. *J. Mol. Biol.* **2004**, *343*, 1019–1034.
20. Lorentzen, E.; Siebers, B.; Hensel, R.; Pohl, E. *Biochemistry* **2005**, *44*, 4222–4229.
21. Shelton, M. C.; Cotterill, I. C.; Novak, S. T. A.; Poonawala, R. M.; Sudarshan, S.; Toone, E. J. *J. Am. Chem. Soc.* **1996**, *118*, 2117–2125.
22. Henderson, D. F.; Shelton, M. J.; Toone, E. J. *J. Org. Chem.* **1997**, *62*, 7910–7912.
23. Fong, S.; Machajewski, T. D.; Mak, C. C.; Wong, C. *Chem. Biol.* **2000**, *7*, 873–883.
24. Wymer, N.; Buchanan, L. V.; Henderson, D.; Mehta, N.; Botting, C. H.; Pocivavsek, L.; Fierke, C. A.; Toone, E. J.; Naismith, J. H. *Structure (Camb)* **2001**, *9*, 1–9.
25. Griffiths, J. S.; Wymer, N. J.; Njolito, E.; Niranjanakumari, S.; Fierke, C. A.; Toone, E. J. *Bioorg. Med. Chem.* **2002**, *10*, 545–550.
26. Bell, B. J.; Watanabe, L.; Rios-Steiner, J. L.; Tulinsky, A.; Lebioda, L.; Arni, R. K. *Acta Crystallogr. D Biol. Crystallogr.* **2003**, *59*, 1454–1458.
27. Nagano, N.; Orengo, C. A.; Thornton, J. M. *J. Mol. Biol.* **2002**, *321*, 741–765.
28. Smith, B. J.; Lawrence, M. C.; Barbosa, J. A. R. G. *J. Org. Chem.* **1999**, *64*, 945–949.
29. Kruger, D.; Schauer, R.; Traving, C. *Eur. J. Biochem.* **2001**, *268*, 3831–3839.
30. Theodossis, A.; Waldden, H.; Westwick, E. J.; Connaris, H.; Lamble, H. J.; Hough, D. W.; Danson, M. J.; Taylor, G. L. *J. Biol. Chem* **2004**, *279*, 43886–43892.
31. Barbosa, J. A. R. G.; Smith, B. J.; DeGori, R.; Ooi, H. C.; Marcuccio, S. M.; Campi, E. M.; Jackson, W. R.;

Brossmer, R.; Sommer, M.; Lawrence, M. C. *J. Mol. Biol.* **2000**, *303*, 405–421.
32. Hertweck, C. *J. Fur Praktische Chemie-Practical Appl. Appl. Chem.* **2000**, *342*, 832–835.
33. Murshudov, G. N.; Vagin, A. A.; Dodson, E. J. *Acta Crystallogr. D Biol. Crystallogr.* **1997**, *53*, 240–255.
34. Bailey, S. *Acta Crystallogr. D Biol. Crystallogr.* **1994**, *50*, 760–763.
35. Jones, T. A.; Zou, J.-Y.; Cowan, S. W.; Kjeldgaard, M. *Acta Crystallogr. A* **1991**, *47*, 110–119.
36. Fradkin, J. E.; Fraenkel, D. G. *J. Bacteriol.* **1971**, *108*, 1277–1283.
37. Griffiths, J. S.; Cheriyan, M.; Corbell, J. B.; Pocivavsek, L.; Fierke, C. A.; Toone, E. J. *Bioorg. Med. Chem.* **2004**, *12*, 4067–4074.
38. Meloche, H. P.; Wood, W. A. *J. Biol. Chem.* **1964**, *239*, 3511–3514.